Estuaries Vol. 28, No. 1, p. 108–123 February 2005

The Influence of Episodic Events on Transport of Striped Bass Eggs to the Estuarine Turbidity Maximum Nursery Area

E. W. NORTH*, R. R. HOOD, S.-Y. CHAO, and L. P. SANFORD

University of Maryland Center for Environmental Science, Horn Point Laboratory, P. O. Box 775, Cambridge, Maryland 21613

ABSTRACT: The estuarine turbidity maximum (ETM) is an important nursery area for anadromous fish where early-life stages can be retained in high prey concentrations and favorable salinities. Episodic freshwater flow and wind events could influence the transport of striped bass (*Morone saxatilis*) eggs to the ETM. This hypothesis was evaluated with regression analysis of observational data and with a coupled biological-physical model of a semi-idealized upper Chesapeake Bay driven by observed wind and freshwater flow. A particle-tracking model was constructed within a numerical circulation model (Princeton Ocean Model) to simulate the transport of fish eggs in a 3-dimensional flow field. Particles with the sinking speed of striped bass eggs were released up-estuary of the salt front in both 2-d event-scale and 60-d seasonal-scale scenarios. In event scenarios, egg-like particles with observed specific gravities (densities) of striped bass eggs were transported to the optimum ETM nursery area after 2 d, the striped bass egg-stage duration. Wind events and pulses in river discharge decreased the number of egg-like particles transported to the ETM area by 20.9% and 13.2%, respectively, compared to nonevent conditions. In seasonal scenarios, particle delivery to the ETM depended upon the timing of the release of egg-like particles. The number of particles transported to the ETM area decreased when particles were released before and during wind and river pulse events. Particle delivery to the ETM area was enhanced when the salt front was moving up-estuary after river pulse events and as base river flow receded over the spawning season. Model results suggest that the timing of striped bass spawning in relation to pulsed events may have a negative (before or during events) or positive (after river flow events) effect on egg transport. Spawning after river flow events may promote early-stage survival by taking advantage of improved transport, enhanced turbidity refuge, and elevated prey production that may occur after river pulse events. In multiple regression analysis of observed data, mean spring freshwater flow rates and the number of pulsed freshwater flow events during the striped bass spawning season explained 71% of the variability in striped bass juvenile abundance in upper Chesapeake Bay from 1986 to 2002. Positive parameter estimates for these effects support the hypothesis that pulsed freshwater flow events, coupled with spawning after the events, may enhance striped bass early-stage survival. Results suggest that episodic events may have an important role in controlling fish recruitment.

Introduction

Estuarine turbidity maxima (ETM) are persistent physical features that can occur at the head of coastal plain estuaries where convergent circulation and tidal scouring at the landward limit of salinity intrusion (i.e., salt front) traps and periodically resuspends sediment (Schubel 1968). The ETM region also is a nursery area for rainbow smelt (*Osmerus mordax*) and tomcod (*Microgadus tomcod*) in the St. Lawrence River (Dodson et al. 1989; Laprise and Dodson 1989; Dauvin and Dodson 1990; Sirois and Dodson 2000; Winkler et al. 2003) and striped bass (*Morone saxatilis*) and white perch (*Morone americana*) in Chesapeake Bay (Boynton et al. 1997; North and Houde 2001). The ETM potentially may be an important larval fish nursery area in the San Francisco Bay-Delta (Jassby et al. 1995; Bennett et al. 2002). In upper Chesapeake Bay, transport of eggs to the ETM nursery area likely is an important component of striped bass life history strategy (North and Houde 2003).

Striped bass are anadromous fish that have important commercial, recreational, and ecological value along the coasts of North America. Striped bass spawn pelagic eggs in tidal freshwater up-estuary of the salt front (Dovel 1971; Secor and Houde 1995; McGovern and Olney 1996; Robichaud-LeBlanc et al. 1996; North and Houde 2001), generally during April and May in Chesapeake Bay (Dovel 1971; Setzler-Hamilton et al. 1981; Rutherford and Houde 1995; Secor and Houde 1995; McGovern and Olney 1996). The spherical eggs are slightly heavier than freshwater (specific gravity = 1.0003–1.0087; Albrecht 1964; Rulifson and Tull 1999; Bergey et al. 2003) and are suspended by currents greater than 0.3 m s^{-1} (Albrecht 1964). Eggs range in size from 1.5 to 4.2 mm depending upon individual spawner and spawning population (Mansueti 1958; Setzler-Hamilton and Hall 1991; Bergey et al. 2003). Striped bass larvae hatch in about 2 d depending upon

* Corresponding author; tele: 410/221-8497; fax: 410/221-8490; e-mail: enorth@hpl.umces.edu

temperature (Mansueti 1958; Doroshev 1970). Although eggs are spawned in freshwater, experimental evidence suggests that survival of earliest-stage larvae can be enhanced in salinities >0 and <9 psu (Albrecht 1964; Lal et al. 1977; Kane et al. 1990; Winger and Lasier 1994).

Transport of eggs to the ETM region may promote survival of larvae because physical circulation patterns may retain larvae in a zone of optimum salinities, abundant zooplankton prey (Simenstad et al. 1994; Boynton et al. 1997; Kimmerer et al. 1998; Roman et al. 2001), and refuge from visual predators in high turbidity waters (Chesney 1989). Retention within the ETM also could prevent eggs and larvae from down-estuary transport and probable mortality (Secor et al. 1995).

Physical conditions and circulation patterns can influence the ETM nursery area on both seasonal and event scales, and may influence the transport and survival of early-stage striped bass. Springtime freshwater flow influences salt front and ETM structure in upper Chesapeake Bay (North and Houde 2001). Spring flow rates are positively correlated with striped bass larval and juvenile abundances (North and Houde 2001, 2003) and with abundances of an important prey of larval striped bass, the copepod *Eurytemora affinis* (Kimmel and Roman 2004). Event-scale processes may be important for early-stage transport and survival. Wind and river pulse events affect circulation patterns near the salt front (Sanford et al. 2001; North et al. 2004). High mortalities of striped bass eggs and larvae have been associated with springtime storm events during the striped bass spawning season (Rutherford and Houde 1995). These mortality events have been ascribed to low water temperatures and low pH (Morgan et al. 1981; Hall et al. 1985; Uphoff 1989; Secor and Houde 1995). The possibility that episodic events also may result in transport of early-life stages away from the ETM nursery area has not been evaluated.

The research presented here was designed to determine if episodic wind or river pulse events that occur during striped bass spawning season could affect the transport of eggs to the ETM nursery area. The potential for wind and river pulse events to contribute to striped bass recruitment variability was evaluated with a regression model using observed wind, river flow, and striped bass spawning stock and juvenile abundance data from upper Chesapeake Bay. A semi-idealized coupled physical-biological model of the ETM region was used to identify the effect of events on striped bass egg transport. The coupled model includes a 3-dimensional (3-D) hydrodynamic model configured to examine along-channel processes in upper Chesapeake Bay and a particle-tracking model to simulate striped bass eggs. Observations of river pulse and wind events in upper Chesapeake Bay were used to parameterize the model. Both event-scale (2-d) and seasonal-scale (60-d) scenarios were conducted to investigate the effect of egg specific gravity (density), release location, and episodic events on the transport of striped bass eggs to the ETM nursery area, and to investigate the cumulative effect of episodic events on transport of eggs to the ETM during an entire spawning season. Combining findings from the regression analysis and numerical model enable us to hypothesize that striped bass may time their spawning in relation to river pulse events to enhance survival.

Multiple Regression Analysis of Observed Data

Methods

Observations of Wind and River Flow Events

Monitoring data were used to determine the frequency and magnitude of wind and river pulse events that occur during the striped bass spawning season (April and May) in upper Chesapeake Bay. This information was used to guide wind and river forcing in model scenarios. Wind velocity data from April and May 1986–2002 at Thomas Point Light in upper Chesapeake Bay (38°53′54″N, 76°26′12″W, see Fig. 1 of North et al. 2004) were derived from the National Oceanic and Atmospheric Administration National Data Buoy Center web page (www.ndbc.noaa.gov). The number, mean wind speed, and duration of down-estuary wind events were calculated. Down-estuary wind events were defined as a period of time ≥12 h during which winds blew from a 90° sector around true north, attained speeds greater than 7.5 m s^{-1} (16.8 mph), and began and ended with speeds greater than 5 m s^{-1} (11.2 mph).

Daily Susquehanna River discharge data at Conowingo Dam (39°39′26″N, 76°10′31″W, see Fig. 1 of North et al. 2004) during April and May 1968–2002 were obtained from the United States Geological Survey (USGS, http://nwis.waterdata.usgs.gov/nwis). The number of peak discharge events during striped bass spawning season was calculated. Peak events were defined as pulses in discharge that were >2 d in duration and exceeded twice the April–May mean discharge for each year.

Statistical Analysis of Juvenile Striped Bass Abundance

A multiple regression analysis was conducted to determine if observed striped bass spawning stock abundance, mean spring freshwater flow rates, and pulsed flow and wind events described a significant amount of variability in observed striped bass juvenile abundances from 1986 to 2002, the duration of the upper Chesapeake Bay spawning stock abun-

dance time series. The index of female striped bass spawning stock abundance in upper Chesapeake Bay was downloaded from the Maryland Department of Natural Resources (MDDNR) Striped Bass Assessment Project web page (see Table 3 at http://www.dnr.state.md.us/fisheries/spring_survey/index.shtml). The abundance index was expressed as catch-per-unit-effort, standardized as the number of female fish captured in 1,000 square yards of experimental drift gill net per hour. An index of striped bass juvenile abundance in upper Chesapeake Bay was downloaded from the MDDNR Striped Bass Seine Survey web page (http://www.dnr.state.md.us/fisheries/juvindex/index.html). This index of young-of-the-year abundance was the arithmetic mean catch per haul of the seine net. Spring freshwater flow rates were the mean of Susquehanna River daily discharge in March, April, and May at Conowingo Dam (USGS). The method for calculating the number of pulsed freshwater flow and wind events per spawning season was described in the previous section. A wind event index was derived for the multiple regression model by adding the number of down-estuary wind events > 21 h in duration with the number of down-estuary wind events > 9.1 m s^{-1} in magnitude. These values are the 75th percentile values for observed duration and mean wind speeds.

A linear multiple regression analysis was conducted with juvenile index as the dependent variable and spawning stock abundance index, mean spring discharge, number of pulsed river flow events, and wind event index as explanatory variables (SAS 8.0, PROC REG, PROC GLM; SAS 1997). Although nonlinear Ricker and Beverton-Holt models have been used to describe the relationship between spawning stock abundance and juvenile recruitment (North and Houde 2003), a linear approach was used because there was no evidence that nonlinear model fit was better than the linear model fit (Ricker adjusted $R^2 = -0.059$, Beverton-Holt adjusted $R^2 = -0.061$, linear model adjusted $R^2 = -0.054$; SAS 8.0, PROC NLIN, PROC MODEL). The linear multiple regression model passed tests for normality (Shapiro-Wilks test) and homogeneity of variance (Pearson correlation tests of |residual| versus predicted values), and did not demonstrate autocorrelation in residuals (SAS 8.0 PROC ARIMA). All explanatory variables passed multicollinearity tests (tolerance > 0.56, condition index = 2.39, SAS 8.0 PROC REG, PROC PRINCOMP). There was no significant correlation between mean spring discharge and the number of pulsed river flow events in each year ($r = 0.30$, $p = 0.23$, SAS 8.0 PROC CORR).

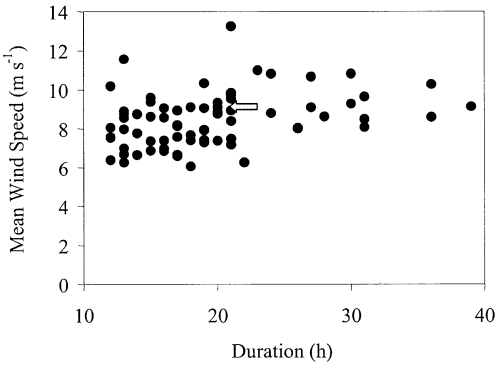

Fig. 1. Mean wind speed (m s^{-1}) versus duration (h) of down-estuary wind events in April and May 1986–2002 in upper Chesapeake Bay measured at Thomas Point Light. The white arrow indicates the duration (21 h) and magnitude (9.1 m s^{-1} wind speed) of down-estuary wind events used in numerical model scenarios.

Results

Observations of Wind and River Flow Events

Results of the observational data analysis indicate that down-estuary wind events occurred frequently during the 1986–2002 striped bass spawning seasons in upper Chesapeake Bay (Fig. 1). The 75th percentile values for duration and mean wind speed were 21 h and 9.1 m s^{-1} (20.4 mph), respectively. Although down-estuary wind events that lasted ≥ 21 h occurred on average 1.47 times per spawning season (SE = 0.34), these events were recorded as many as 5 times and as few as zero in any given year. Down-estuary wind events with speeds ≥ 9.1 m s^{-1} occurred on average 1.24 times per spawning season (SE = 0.29), but happened as many as 4 times and as few as zero in any given year.

Susquehanna River discharge data indicated that large pulses in river flow consistently occurred during the 1968–2002 striped bass spawning seasons in upper Chesapeake Bay (Fig. 2). On average, peak discharge events occurred once per spawning season (mean = 1.00, SE = 0.12), although as many as 3 peak discharge events or as few as zero could occur.

Statistical Analysis of Juvenile Striped Bass Abundance

Results of the multiple regression analysis indicate that mean spring freshwater discharge and the number of pulsed freshwater flow events during the spawning season explained a significant amount of the variability in the 1986–2002 juvenile striped bass abundance index in upper Chesapeake Bay (adjusted $R^2 = 0.70$, Table 1). Regression parameter estimates and scatter plots (Fig. 3) indicate that mean spring discharge (partial $r^2 = 0.50$) and the number of pulsed flow events (par-

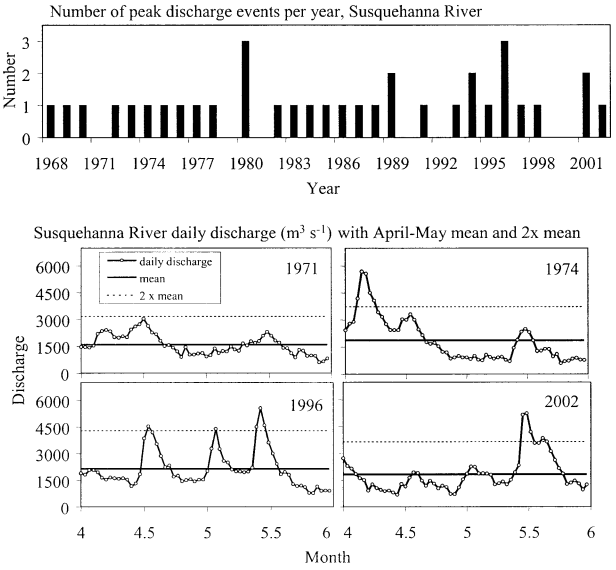

Fig. 2. Number of peak discharge events per year during April and May for Susquehanna River measured at Conowingo Dam. Peak events were defined as spikes in discharge that lasted more than 2 d and exceeded twice the April–May mean discharge. Susquehanna River daily discharge during April and May for selected years (year labeled in upper right corner of each panel). Horizontal lines indicate mean discharge in April and May (thick solid) and twice the mean discharge (thin dashed).

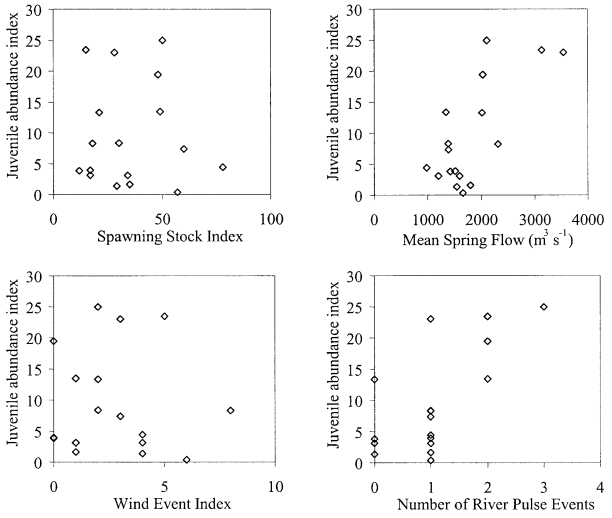

Fig. 3. Scatter plots of data from 1986–2002 in upper Chesapeake Bay. Plots contain striped bass juvenile abundance index (catch per seine haul) versus striped bass spawning stock abundance index (number of female fish captured per square yard of experimental drift gill net per hour), mean Susquehanna River freshwater discharge in March, April, and May, an index of down-estuary wind events during striped bass spawning season (April and May), and the number of peak river flow events that occurred during striped bass spawning season.

tial $r^2 = 0.35$) were positively related to the index of juvenile abundance. Spawning stock abundance and wind event indices were not significant in the regression model. When these variables were removed, the model with mean spring freshwater discharge and the number of pulsed flow events explained 71% of the variability in upper Chesapeake Bay juvenile abundance.

Description of Numerical Models

Hydrodynamic Model

A semi-idealized hydrodynamic modeling framework was selected to isolate first-order physical processes that could affect striped bass egg transport. Our focus was on longitudinal processes and the relationship between pulsed events, salt front structure, and egg-like particle transport. The numerical model was scaled to match upper Chesapeake Bay characteristics based on predicted tides and field studies (North and Houde 2001; Sanford et al. 2001; North et al. 2004).

The 3-D hydrodynamic ETM model was based on the code of the Princeton Ocean Model (POM) under hydrostatic and Boussinesq approximations (Blumberg and Mellor 1987; Mellor 1998) with eddy viscosity and diffusivity determined by the level-2.5 turbulent closure scheme of Mellor and Yamada (1974). Detailed information about hydrodynamic model parameterization, boundary conditions, and our enhancements to POM can be found in North et al. (2004). Our enhancements included building suspended sediment and sediment transport components, adding constant loading of suspended sediment at the up-stream boundary, parameterizing bottom sediment burial with a Newtonian dampening term, and constructing a more reasonable formulation for background

TABLE 1. Multiple regression analysis results. The dependent variable in the analysis was an index of upper Chesapeake Bay striped bass juvenile abundance in 1986–2002. Model adjusted $R^2 = 0.70$. Adjusted $R^2 = 0.71$ when spawning stock abundance and wind event index were removed from the model.

Explanatory Variable	Parameter Estimate (SE)	Degrees of Freedom	F Value	Pr > F	Partial r^2
Spawning stock abundance	0.009 (0.08)	1	0.01	0.911	0.001
Mean spring freshwater flow	0.008 (0.002)	1	11.82	0.005	0.50
Number of river pulses	4.67 (1.85)	1	6.36	0.027	0.35
Wind event index	−0.63 (0.56)	1	1.27	0.281	0.10

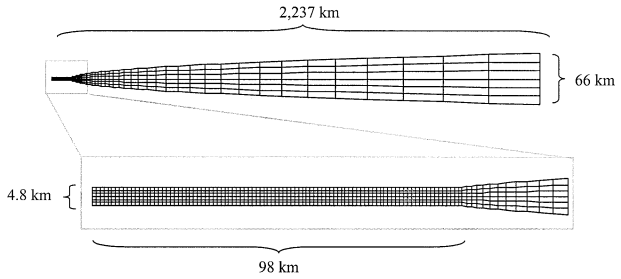

Fig. 4. Schematic of model domain. Upper diagram represents the entire model domain. Lower diagram illustrates the grid line geometry of the channel, the region of interest. Reproduced from North et al. 2004.

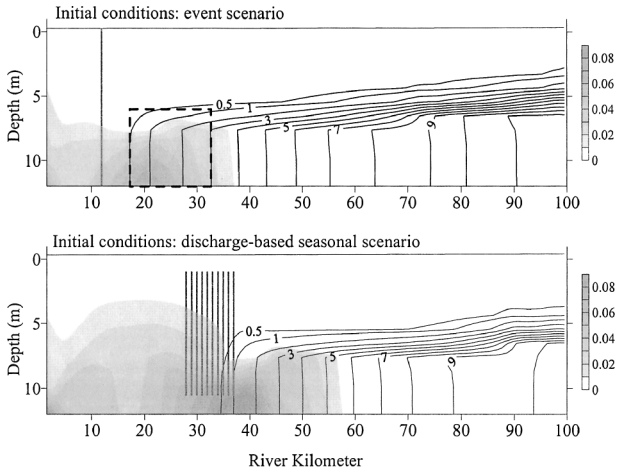

Fig. 5. Along-channel section of hydrodynamic model output with salinity (psu) line contours and suspended sediment shaded contours (kg m^{-3}). Steady-state solution and initial conditions for 2-d event scenarios are shown in the upper panel. Dashed box indicates region of optimum ETM nursery area. Gray line indicates release location of particles at river kilometer 12. Initial conditions for 60-d discharge-based seasonal scenarios are shown in the lower panel. Gray lines indicate release locations of first cohort of egg-like particles.

vertical diffusivity to better represent vertical diffusivity under strongly stratified conditions.

The ETM model domain (Fig. 4) contained a 98-km long and 4.8-km wide channel with a gradually widening seaward reservoir that was 2,237-km long and had a maximum width of 66 km. The entire basin contained 145 grid spacings in the x-direction (seaward) and 6 in the y-direction (across channel) and was 12 m deep. Vertical resolution was provided by 12 sigma-coordinate layers. In the channel, the longitudinal resolution (Δx) was 1 km and the lateral resolution (Δy) was 0.8 km. In the seaward reservoir, Δx and Δy gradually increased at a rate of 12 and 5.5 percent per grid, respectively. The seaward reservoir, although of minor importance to the circulation and sediment transport within the channel, enhanced the long-term computational stability of the model. The temporal resolution of the model was split. Vertically averaged currents and sea level were resolved with a time step of 5 s. Salinity, sediment concentration, and vertically explicit current velocities were resolved with a time step of 40 s.

Semidiurnal tidal currents in the channel were produced with a barotropic tidal generation force in the longitudinal momentum equation. Tidal current speed and an upstream dissipation parameter were adjusted so that sea level heights and tidal current velocities in the model were similar to those of predicted tides in upper Chesapeake Bay. To focus on longitudinal processes, the lateral walls bounding the channel were impenetrable, impermeable, and free-slip, the Coriolis force was removed from momentum equations, and coefficients of horizontal viscosity and diffusivity were prescribed as constants instead of varying with local flow divergence and vorticity.

Initially, the model channel was filled with motionless clear water of 20°C and 12 psu, and no sediment was at the bottom of the basin. The model was run with constant river inflow (0.07 m s^{-1}) of 0 psu, constant temperature (20°C), and constant sediment loading at the up-estuary boundary until the model reached a quasi steady state at day 350 (Fig. 5). In this quasi steady state, sediment input equaled sediment burial and the location of the salt front was stable; the salt front oscillated with the tidal currents in a repetitive cycle but did not progress up or down the estuary. All model scenarios used the quasi steady-state solution at day 350 as the initial condition.

Particle-tracking Model

The Lagrangian particle-tracking model was constructed as a subroutine of the hydrodynamic model that was called every internal time step (40 s). Current velocity, sea surface height, water density, and vertical diffusivity derived in the hydrodynamic model were passed to the particle-tracking model. Changes in particle locations due to advection and sinking were calculated every 10 s using a water column profile interpolation scheme (see below) to estimate current velocity and water density at each particle location. Near the bottom, the law-of-the-wall was applied so that u, v, and w current velocities decreased logarithmically to the depth of the roughness height (0.001 m). Changes in the vertical location of particles due to subgrid scale turbulence were updated every 1 s using a random displacement model (see below).

Interpolation Scheme

In the water column profile interpolation scheme, modeled velocities, water density, and dif-

fusivities were interpolated horizontally (4-point linear interpolation) at each sigma level to create a vertical profile of values at the x-y particle location. For current velocities and water density, a tension spline curve was fit to the vertical profile and was used to estimate current velocity or water density at the particle location (except near the bottom where the law-of-the-wall was applied for current velocities). To implement the random displacement model to simulate turbulent particle motion (see below), two steps were added to the water column profile interpolation scheme to estimate vertical diffusivity (K_v) and its derivative (K_v') at the particle location. After the water column profile of vertical diffusivity at the x-y particle location was constructed, the number of data points between sigma layers was proliferated with linear interpolation. An 8-point moving average was used to smooth the data before fitting the tension spline curve to the profile of vertical diffusivity, from which K_v' can be determined.

The water column profile interpolation scheme reduces numerical artifacts that can occur in particle-tracking models. Without it, sinking particles tend to aggregate on sigma levels prescribed by the hydrodynamic model. When the random displacement model is implemented to account for subgrid scale turbulence, the water column profile interpolation scheme prevents artificial aggregation of particles in regions of sharp gradients in diffusivity.

Subgrid Scale Turbulence

Unlike random walk models, random displacement models do not result in numerical artifacts (particle aggregation in regions of low diffusivity) if the vertical resolution is adequate to resolve sharp variations in vertical diffusivity (Visser 1997; Brickman and Smith 2002). A random displacement model (Visser 1997) was implemented within the particle-tracking model to simulate subgrid scale turbulence in the vertical (z) direction:

$$z_{n+1} = z_n + K'_v\delta t + R(2r^{-1}K_v\delta t)^{1/2} \qquad (1)$$

where z_n = initial particle location, K_v = vertical diffusivity evaluated at $(z_n + 0.5K_v'\delta t)$, δt = time step of the random displacement model, K_v' = $\partial K_v/\partial z$ evaluated at z_n, and R is a random number generator with mean = 0 and standard deviation r = 1. To satisfy the random displacement model criterion $\delta t \ll \min(1/K_v'')$ (Visser 1997), the time step (δt) was set at 1 s after examination of a 10-d time series of $1/K_v''$ that included wind events. When $K_v' = 0$, the random displacement model (Eq. 1) reduces to a random walk model (Visser 1997).

We modeled subgrid scale turbulence in the vertical but not the horizontal because the particle-tracking model resolved vertical shear dispersion, which is the dominant along-channel mixing process in straight estuaries (Geyer and Signell 1992), and because an estimate of realistic horizontal diffusivity indicated that it was very small compared to the total horizontal diffusivity used in the hydrodynamic model (< 0.1% based on Eq. 20 in Sanford et al. 1992). Horizontal diffusivity in the 3-D hydrodynamic model was set at a constant value to avoid model instability and does not necessarily reflect realistic mixing at the time scale of the particle-tracking model.

Particle Sinking Speeds

Reynolds numbers for striped bass eggs are between 3 and 4 based on egg settling velocity and diameter measurements made by Schubel et al. (1974). Because Stokes Law does not apply when Reynolds numbers are > 1, we used a series of equations that describe the sinking speed of spherical particles at Reynolds numbers < 800 (Raudkivi 1990). Stokes Law was used to approximate egg sinking speed (w_s):

$$w_s = \frac{gd^2(\rho' - \rho)}{18\rho\nu} \qquad (2)$$

where g = gravity, d = diameter of sphere, ρ' = density of sphere, ρ = density of water, and ν = kinematic viscosity (1.2×10^{-6} m^2 s^{-1}). Water density at the particle location was derived from hydrodynamic model output. The Stokes sinking speed estimate was used to calculate the Reynolds number (Re):

$$Re = w_s d\nu^{-1} \qquad (3)$$

which then was used to calculate drag coefficient (C_d) using the Schiller and Naumann (1933) empirical equation for C_d at Re < 800:

$$C_d = \frac{24(1 + 0.15Re^{0.687})}{Re} \qquad (4)$$

Initial values of Re and C_d were inserted into the generalized terminal velocity equation:

$$w_s = \left[\frac{4gd(\rho' - \rho)}{3C_d\rho}\right]^{1/2} \qquad (5)$$

Equations 3, 4, and 5 were iteratively solved until the sinking speed converged to a single value to produce a valid estimate of sinking speed at Reynolds numbers < 800 (Raudkivi 1990). This method was used to calculate the sinking speed of each particle at every time step (10 s).

The effect of water density on the sinking of egg-like particles was due to salinity alone because temperature was constant throughout the model domain. Salinity is the main determinant of water

density near the salt front and the primary water characteristic that affects striped bass egg sinking. Salinity can account for 80–94% of the density difference between 0 and 3 psu at temperatures observed in the upper Chesapeake Bay salt front during striped bass spawning season.

Boundary Conditions

If turbulence or vertical advection caused a particle to pass through the surface or bottom boundary, the particle was placed back in the model domain at a distance from the boundary equal to the distance that the particle location exceeded the boundary (i.e., it was reflected). If sinking caused a particle to pass through the bottom boundary, the particle was placed in the model domain 1.25 mm from the boundary (the distance equal to the radius of a striped bass egg).

Model Scenarios

Model scenarios were developed to examine the influence of egg specific gravity, spawning location, and river flow and wind events on transport of egg-like particles to the optimum ETM nursery area. The optimum ETM nursery area was defined as the low salinity area (0.5–3 psu) at the foot of the salt front (waters deeper than 6.0 m; Fig. 5) where early-life stages could be retained in an area of high prey concentrations (Simenstad et al. 1994; Kimmerer et al. 1998; Roman et al. 2001; North and Houde 2003) and low salinities favorable for striped bass larval survival (Albrecht 1964; Lal et al. 1977; Kane et al. 1990; Winger and Lasier 1994).

To simulate striped bass eggs, particle diameter was fixed at 2.5 mm to isolate the effects of egg specific gravity, spawning location, and water density on transport of egg-like particles to the ETM. This diameter is the mean egg diameter from 9 populations of striped bass (see Table 2 of Bergey et al. 2003). Release location of egg-like particles was at or up-estuary of the salt front because striped bass eggs have been found to peak between 0 and 10 km from the intersection of the 1 psu isohaline with the bottom (Robichaud-LeBlanc et al. 1996; North and Houde 2001). Because striped bass eggs hatch in approximately 2 d (Mansueti 1958; Doroshev 1970), the number of particles suspended in the ETM nursery area were counted 2 d after release. Although striped bass egg hatching times vary depending upon temperature, we used one value for egg stage duration in the model in order to isolate the effects of egg specific gravity, release location, and water density on egg transport, and because temperature was constant throughout the model domain. Particles that were transported down-estuary of the optimum ETM nursery area were considered lost. Likewise, particles that sunk to the bottom (where eggs can be smothered by sediment) and were located within 2.5 mm of the bottom at the end of the 2-d period were considered lost.

Short-term Event Scenarios

Short 2-d event scenarios were conducted to investigate the effect of egg specific gravity, release location, and wind and river pulse events on the transport of striped bass eggs to the ETM. In each model run, 1,000 egg-like particles were released throughout the water column of the hydrodynamic model on day 350 and tracked for 2 d (until hatching). At day 352, the number of particles in the optimum ETM nursery area was enumerated. Specific gravities and release locations of particles were varied between model runs. Egg specific gravities ($sg = \rho' \rho^{-1}$) were assigned in increments of 0.0002 (from 1.0001 to 1.0014) or 0.0005 (from 1.0015 to 1.004). Release locations occurred throughout the water column (Fig. 5) and were stepped in increments of 2 km from 0 to 10 km up-estuary of the 1 psu isohaline. The suite of 78 model runs (13 specific gravities $\times$ 6 release locations) was conducted with the hydrodynamic model in steady state, river pulse, and wind event scenarios for a total of 234 model runs and 234,000 particles released.

Observed wind and river events served as a guide to parameterize the wind event and river pulse simulations. The 75th percentile values for duration (21 h) and mean wind speed (9.1 m s^{-1}) were chosen to parameterize modeled wind events so that scenarios would mimic strong events during striped bass spawning season that occurred with regular frequency. To simulate the wind event, a 1.66 dyne cm^{-2} down-estuary wind stress (corresponding to 9.1 m s^{-1} wind speed) was applied to the sea surface from day 351.125 until day 352 (i.e., 21 h). River pulse events in the numerical model were simulated by doubling the steady-state river inflow rate (i.e., from 0.07 to 0.14 m s^{-1}) from day 350 to day 352.

Seasonal Scenarios

Long-term 60-d seasonal scenarios were conducted to investigate the cumulative effect of episodic events on transport of striped bass eggs to the optimum ETM nursery area during an entire spawning season. Two suites of model runs were conducted: steady state and discharge based. In steady-state scenarios, river inflow remained constant (0.07 m s^{-1}) for the duration of the 60-d simulations. In discharge-based scenarios, river inflow increased then decreased to simulate springtime river flows during striped bass spawning season

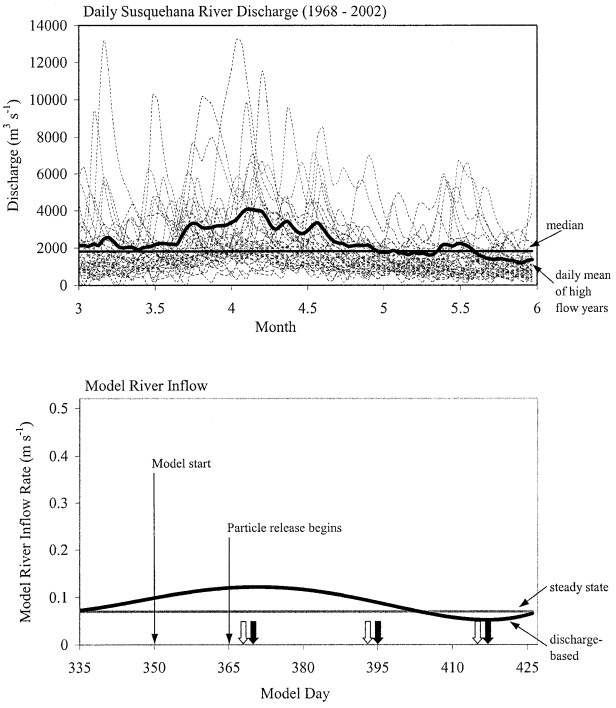

Fig. 6. Parameterization of 60-d seasonal model scenarios. Observed daily Susquehanna River discharge ($m^3 s^{-1}$) during March, April, and May 1968–2002 (thin hatched lines) with median (flat black line) of March–May mean discharge are in the upper panel. Mean daily discharge of high flow years (upper 50th percentile) is illustrated by the thick black line. Model steady-state (flat line) and discharge-based (thick black line) inflow rates are in the lower panel. The latter is a 4th-order polynomial fit to observed daily mean flow rates from upper 50th percentile flow years (thick black line) in panel and scaled so that modeled and observed flow rates were proportional. Arrows indicate the start time of 21-h wind (white arrow) and 2-d river pulse (black arrow) events.

(Fig. 6). USGS daily Susquehanna River discharge ($m^3 s^{-1}$) data during March, April, and May (1968–2002) were used to construct the discharge-based river inflow rates. Mean March–May flows were calculated for each spawning season, and the median (flat line in Fig. 6) and upper 50th percentile spawning season flow rates were determined. A time series was constructed by calculating the daily mean discharge from the upper 50th percentile spawning seasons (thick curved line in Fig. 6). This time series, smoothed by a 4th-order polynomial, was used to develop the discharge-based model inflow rates. Model river inflow rates were scaled so that the difference between steady-state inflow rates (flat line, Fig. 6, lower panel) and discharge-based inflow rates (curved line, Fig. 6, lower panel) were proportional to the difference between the median spawning season flow rate (flat line, Fig. 6, upper panel) and daily mean discharge time series from upper 50th percentile spawning seasons (thick curved line, Fig. 6, upper panel).

In the seasonal scenarios, either steady-state or discharge-based river inflow commenced on day 350 corresponding to March 15 in the discharge record (Fig. 6). Starting on day 365 (corresponding to April 1 in the discharge record), batches of egg-like particles were released every 24 h for 60 d in a grid spanning 0 to 10 km up-estuary of the 1 psu isohaline (Fig. 5). In each 24-h batch, 1,000 uniformly distributed particles were assigned specific gravities (densities) of 1.0005, 1.0011, and 1.002, for a total of 3,000 particles. These specific gravities were chosen because they represent the range of specific gravities that result in the most particles transported to the optimum ETM nursery areas in the 2-d event scenarios. Egg-like particles in each 24-h batch were tracked for 2 d at which time the number of particles in the optimum area was enumerated.

To investigate the influence of wind and river flow events on striped bass egg transport, model runs were conducted with events and compared to model runs without events. For the event simulations, three springtime storms were simulated near the beginning, middle, and end of the 60-d model run. Three storms were simulated because the maximum number of river pulse events observed during striped bass spawning seasons was three. Each storm included a 21-h down-estuary wind event (wind stress = 1.66 dyne cm^{-2}) followed 1.125 d later by a 2-d river pulse event during which river inflow rates were 0.14 m s^{-1}, twice the steady-state inflow rate. Storms were initiated on model days 368, 393, and 415 corresponding to April 2, April 27, and May 19 in the discharge record (see Fig. 6 for event timing). Particle release occurred before, during, and after the events because batches of egg-like particles were released daily in the seasonal scenarios.

The following model runs were conducted: steady state with no events, steady state with events, discharge based with no events, and discharge based with events. In each model run, 180,000 particles (3,000 d^{-1} for 60 d) were released for a total of 720,000 particles released in the seasonal scenarios.

Number of Particles

The number of particles used in the above scenarios was determined by examining the mean and variance of model results versus number of particles released. Ten 2-d wind event scenario model runs were conducted with identical models (the same physical conditions, number of particles, particle specific gravity [1.0005], and particle release location [14 river kilometer]), except that differ-

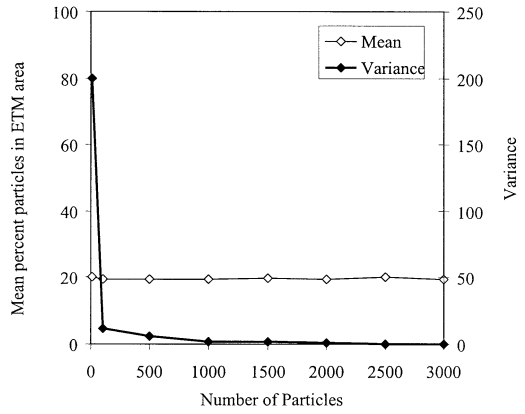

Fig. 7. Variance and mean of Lagrangian model solution versus number of particles released. Each data point summarizes 10 model runs that were identical except different seed values were used to initialize the random number generator in the subgrid scale turbulence model. Percent particles found in the optimum ETM nursery area after 2 d in each model run were used to construct the mean and variance. Particles were released at river kilometer 14, assigned a specific gravity of 1.0005, and subjected to a 21-h down-estuary wind event (1.66 dyne cm^{-2} wind stress).

ent seed values were used to initialize the random number generator in the subgrid scale turbulence model. The 10 model runs were conducted with 10, 100, 500, 1,000, 1,500, 2,000, 2,500, and 3,000 particles. The lowest number of particles that resulted in minimal variance was selected (1,000 particles; Fig. 7).

Numerical Model Results

Short-term Event Scenarios

Results of the 2-d scenarios in steady-state conditions indicated that transport of egg-like particles to the optimum nursery area depended on release location and egg specific gravity (Fig. 8). Although all release locations resulted in delivery of some egg-like particles to the optimum nursery area after 2 d of steady-state conditions, most (95.8%) successful releases occurred between 6 and 0 km from the 1 psu isohaline (at 14, 16, 18, and 20 river kilometers). Most egg-like particles (86.1%) located in the optimum area had specific gravities between 1.0005 and 1.002 (e.g., snapshot of particle distribution with sg = 1.0007 in Fig. 9). Egg-like particles with low specific gravities floated over the salt front and were transported down-estuary (e.g., snapshot of particle distribution with sg = 1.0001), whereas those with relatively high specific gravities sunk to the bottom where they remained (e.g., particles with sg = 1.004).

River pulse and wind events affected circulation patterns in the modeled ETM region (Fig. 9). Compared to steady-state conditions, the down-estuary wind event resulted in a 4.5-km down-estuary shift in salt front location, a longitudinal compression of the salt front (0.5 and 3 psu isohalines were closer together), and enhanced mixing of low salinity waters in the upper water column. The 2-d river pulse event also shifted the salt front down-estuary (by 6.3 km) and compressed the optimum nursery area longitudinally, but did not enhance salinity mixing. Stratification was intensified and down-estuary current velocities in surface waters (not shown) were enhanced.

Episodic events also influenced the transport of egg-like particles to the optimum ETM nursery area. Wind events resulted in a 20.9% reduction in the total number of egg-like particles delivered to the optimum area compared to steady-state conditions (Table 2, Fig. 8). Low and high specific gravity particles were preferentially lost, failing to reach the ETM nursery area. The lightest particles were mixed up into surface waters and transported down-estuary while the heaviest particles remained near the bottom and did not travel down-estuary with the salt front (Fig. 9). Of the particles found in the optimum area, most had specific gravities between 1.0005 and 1.002 (95.9%), and most (84.5%) were released between 14 and 20 river kilometers (within 6 km upstream of 1 psu isohaline before wind).

River pulse events resulted in a 13.2% reduction in the total number of egg-like particles transported to the optimum ETM nursery area compared to steady-state conditions (Table 2). Similar to the wind-induced perturbation, low and high specific gravity particles were less favorably retained in the optimum area (Fig. 8). The lightest particles were transported down-estuary over the salt front while heaviest particles remained near the bottom and did not travel as quickly down-estuary as did the salt front (Fig. 9). Of the particles found in the optimum area, most had specific gravities between 1.0005 and 1.002 (99.3%), and most were released between 14 and 20 river kilometers (80.0%). Compared to steady-state conditions, more particles released farther up-estuary (10 and 12 river kilometers) were delivered to the ETM area in river pulse scenarios. This up-estuary shift in suitable release locations was also observed in wind event scenarios.

Seasonal Scenarios

Changes in river inflow and wind affected the location of the salt front and ETM over time (Fig. 10). In the discharge-based scenarios, the optimum ETM nursery area moved with the salt front (Fig. 5) as the front progressed approximately 18 km down and then 27 km up-estuary with increasing and then decreasing freshwater flow (Fig. 10). In steady-state scenarios, the salt front remained at,

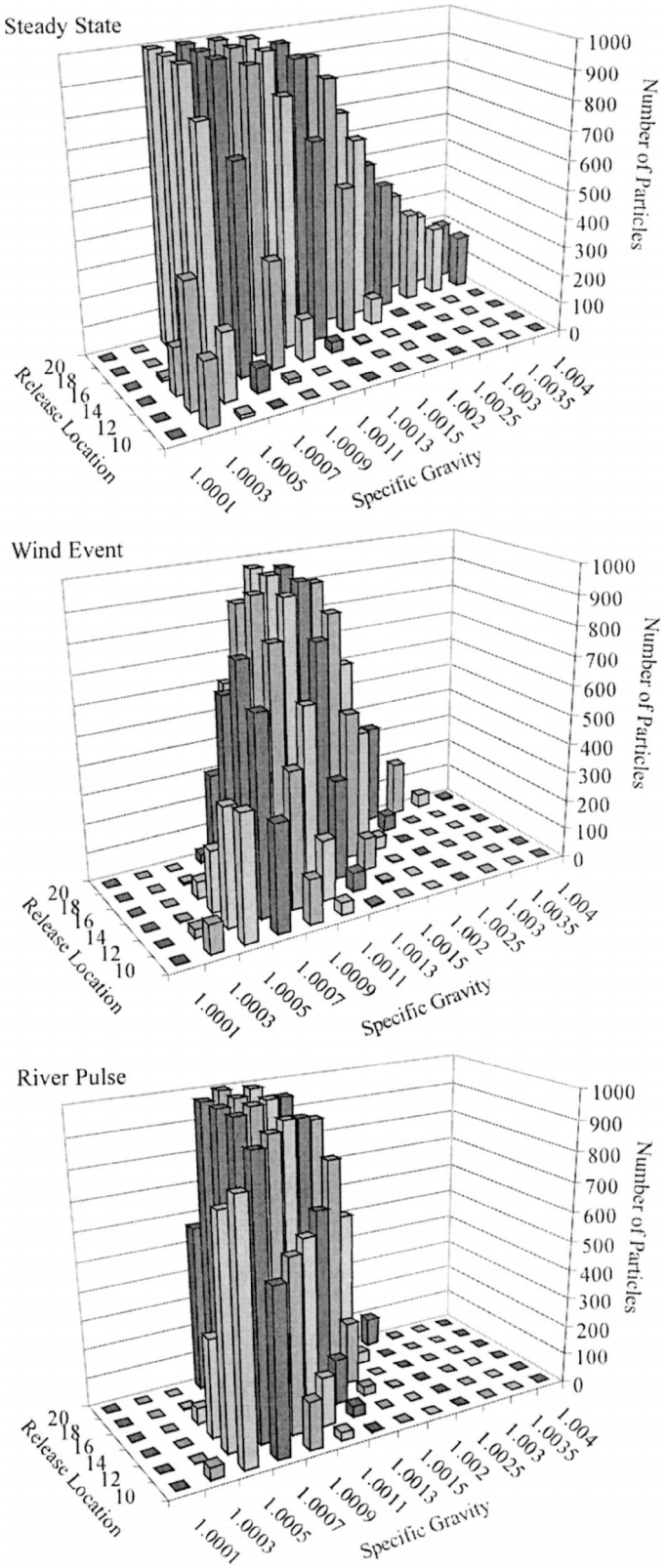

Fig. 8. Number of egg-like particles in the optimum ETM nursery area after 2 d as a function of release location (km) and egg specific gravity (density) in steady state, wind event, and river pulse scenarios.

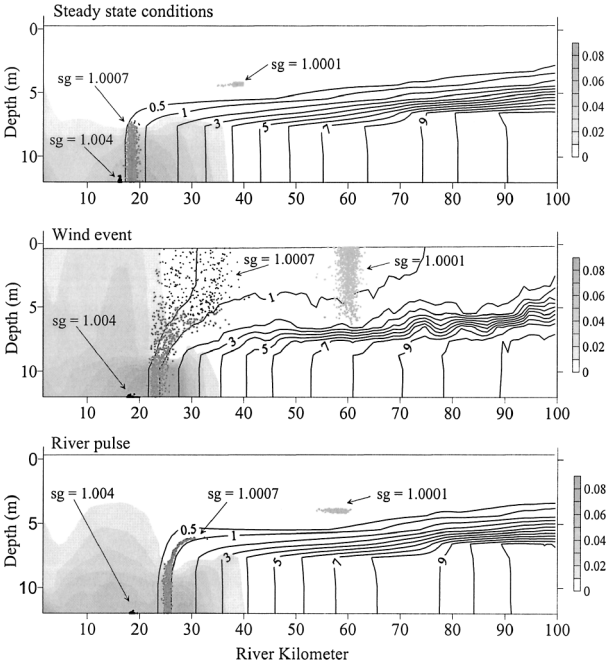

Fig. 9. Salinity (psu, line contours), suspended sediment concentrations (kg m^{-3}, shaded contours), and distribution of striped bass egg-like particles 2 d after release throughout the water column at river kilometer 16 in steady state, wind event, and river pulse conditions. The locations of 3 sets of egg-like particles are depicted in each panel, those with specific gravities (sg) of 1.0001 (light gray), 1.0007 (dark gray), and 1.004 (black).

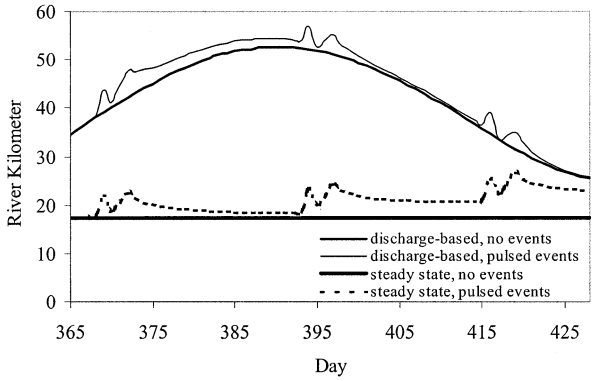

Fig. 10. Location of the salt front (intersection of the 0.5 psu isohaline with the bottom) over time for steady-state (lower lines) and discharge-based (upper lines) scenarios without wind events and river pulses (smooth lines) and with them (lines with small peaks).

or within 9 km, of the initial salt front location. The response of the salt front to events was similar in steady-state and discharge-based scenarios. Wind events caused an initial down-estuary movement of the salt front, followed by an up-estuary shift. The up-estuary response was likely a depth-dependent response to lowered sea surface height in the upper estuary (North et al. 2004). The subsequent pulse in river flow resulted in down-estuary movement of the salt front and was followed by another up-estuary shift after the pulse was complete.

Of the 180,000 particles released, most were transported to the optimum ETM nursery in all scenarios, as was expected based on the range of specific gravities prescribed. In scenarios without events, the total number of egg-like particles was slightly lower in steady-state (60.4%) than in discharge-based scenarios (63.9%; Table 3). In the discharge-based scenario, fewer egg-like particles were found in the optimum area when the salt front was advancing down-estuary compared to steady-state results, and more were found when the salt front was retreating up-estuary (Fig. 11).

The total number of egg-like particles transported to the optimum ETM nursery area for the entire spawning season was similar between models with and without events (Table 3, Fig. 11). In steady-state scenarios, 60.4% of particles were transported in nonevent conditions compared to 60.6% in the model with events. In discharge-based scenarios, 63.9% of particles were transported in nonevent conditions compared to 63.5% in the model with events. In both scenario types, the obvious decrease in the number of egg-like particles in the ETM nursery area during the wind and river pulse events was balanced by an increased number of particles delivered to the optimum area just after the river pulse event. Although the increase in particle transport after the river pulse event was more variable in the discharge-based scenario, results of both scenario types suggest that the up-estuary movement of the salt front after a pulse in

TABLE 2. Summary statistics for 2-d event scenarios.

	Steady State	Wind Event	River Pulse
Total number of eggs released	78,000	78,000	78,000
Number of eggs in optimum ETM nursery area			
Total number	23,801	18,821	20,653
Percent	30.5%	24.1%	26.5%
Mean (± 1 SE)	305 (44)	241 (38)	265 (44)
Percent reduction compared to steady-state conditions	—	20.9%	13.2%

TABLE 3. Summary statistics for 60-d spawning season scenarios.

	Steady State		Discharge Based	
	No Events	Events	No Events	Events
Total number of eggs released	180,000	180,000	180,000	180,000
Number of eggs in optimum ETM nursery area				
Total number	108,777	109,062	114,957	114,291
Percent	60.4%	60.6%	63.9%	63.5%
Mean (± 1 SE)	1,813 (4)	1,818 (28)	1,916 (34)	1,905 (37)

discharge promoted egg-like particle transport to the optimum ETM nursery area.

Discussion

Model results suggest that striped bass egg specific gravity and location of adult spawning may be adapted to optimize transport of eggs to the ETM nursery area. Observations of freshwater flow and wind demonstrate that events occur regularly during the striped bass spawning season in upper Chesapeake Bay. In model scenarios, pulsed events had a negative effect on transport of egg-like particles to the optimum ETM nursery area when particles were released just before and during the events. Favorable transport of egg-like particles to the ETM nursery area occurred if particles were released when the salt front was retreating up-estuary, either on event or seasonal time scales. Results of the multiple regression analysis indicated that pulses in river flow during the spawning season may enhance early-stage survival. Field observations and modeling results combined suggest that striped bass may spawn after pulses in river flow to take advantage of physical and biological conditions that could promote early-stage survival.

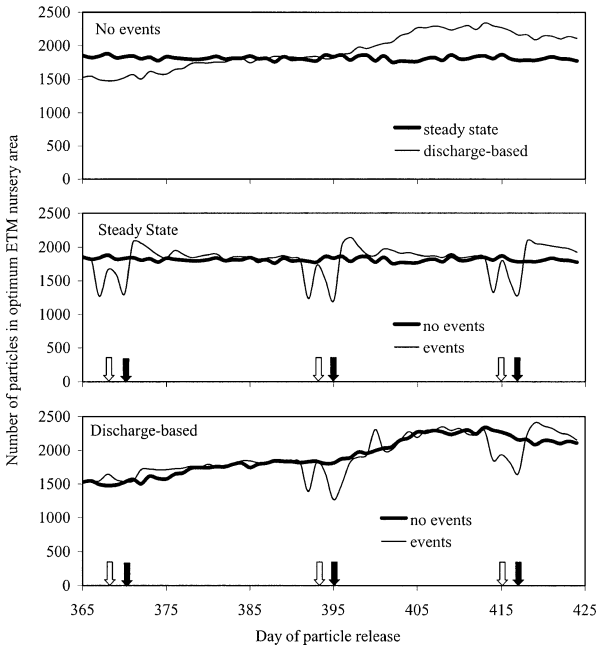

Fig. 11. Number of egg-like particles in optimum nursery area versus time (day on which particles were released) in steady-state and discharge-based scenarios with no episodic events, steady-state scenarios with and without wind and river pulse events, and discharge-based scenarios with and without wind and river pulse events. Arrows indicate the start time of 21-h wind (white arrow) and 2-d river pulse (black arrow) events.

Striped bass egg characteristics (size, specific gravity) and spawning location (up-estuary of the salt front) may be adaptations that promote egg transport to the ETM nursery area. In the 2-d event scenarios, the number of egg-like particles in the optimum area depended upon egg specific gravity and release location. Most egg-like particles delivered to the ETM nursery area had specific gravities between 1.0005 and 1.002 and were released between 0 and 6 km up-estuary of the intersection of the 1 psu isohaline with the bottom. Peak concentrations of striped bass eggs have been found within 0–10 km up-estuary of the salt front (Robichaud-LeBlanc et al. 1996; North and Houde 2001). Modeled specific gravities were within the range observed for striped bass eggs: 1.0003 to 1.0087 (Albrecht 1964; Rulifson and Tull 1999; Bergey et al. 2003). The agreement between model results and observations suggests that spawning up-estuary of the salt front and egg transport to the ETM nursery area may be an important component of striped bass early-life history.

Striped bass egg characteristics may be adapted to specific river systems to optimize transport of eggs to nursery areas. Significant genetic differentiation between striped bass populations along the western Atlantic coast suggests that striped bass have homing fidelity (i.e., adults return to natal systems to spawn; Waldman et al. 1996). A comparative study of eggs from different Atlantic coast populations indicated that eggs were heavier and larger in high-energy river systems than those found in low-energy river systems (Rulifson and Tull 1999; Bergey et al. 2003). Kinetic energy in an estuarine system is related to the magnitude of tidal velocities and freshwater flow velocities, both of which could affect egg transport to nursery ar-

eas. The egg characteristics (specific gravity, diameter) produced by striped bass populations may be adapted for transport to important nursery areas (like ETM) and may vary among spawning populations because tidal and freshwater flow velocities differ among systems.

Model results indicate that egg transport to the ETM nursery area may be optimal in the latter part of the spawning season when river flow recedes. In discharge-based scenarios, the salt front and ETM moved up-estuary as river flow decreased during the later half of the spawning season. At this time, egg-like particle transport to the ETM increased. This general pattern in salt front-ETM movement, coupled with spawning up-estuary of the salt front and retention of larvae within it (North and Houde 2001, 2003), may explain field observations that highest striped bass egg concentrations tended to occur further upriver as the season progressed (Rutherford et al. 1997) and that peak larval concentrations shifted up-estuary over the spawning season (Setzler-Hamilton et al. 1981).

River pulse and wind events are an important characteristic of striped bass spawning seasons in upper Chesapeake Bay. Our analysis of observational data showed that peak river flow events occur on average once per spawning season and range in occurrence from 0 to 3 times. Strong down-estuary wind events take place on average 1.24 times per spawning season, and can occur between 0 and 4 times. Storm events have been observed during striped bass spawning seasons in Chesapeake Bay (Rutherford and Houde 1995; North and Houde 2001), and our results demonstrate that these events are a regular component of environmental conditions during the spawning season. Preliminary analysis suggests that up-estuary wind events may also occur with regular frequency and would be important to include in future investigations because up-estuary wind events can change the circulation and salt front structure of the ETM and potentially affect egg transport (North et al. 2004).

Short-term (2-d) changes in physical conditions affected circulation patterns and egg-like particle transport in the coupled biological-physical model. In total, modeled river pulse and wind events resulted in a reduction (20.9% and 13.2%, respectively) in the number of egg-like particles in the optimum ETM nursery area compared to steady-state conditions. In all simulations, down-estuary wind events, pulses in river flow, and seasonal-scale increases in river inflow (not shown) compressed the isohalines within the salt front. Although this compression reduced the size of the optimum area (defined as the region between the intersection of 0.5 and 3 psu with the bottom), it did not have a significant effect on model results. If the ETM nursery area was defined as a fixed region between the 0.5 psu intersection and 15 km down-estuary, the percent of total particles transported to this area in 2-d event scenarios was 30.5% in steady-state conditions, 24.5% after the wind event, and 26.7% after the river pulse. These values are similar to the percentages reported in Table 2: 30.5% (steady state), 24.1% (wind event), and 26.5% (river pulse). Compression of the salt front did not confound model results because the most critical regions affecting egg-like particle disposition were up-estuary of the salt front, along the face of the front, and within the pycnocline, not in the interior of the front between 1 and 3 psu. Wind and river pulse events resulted in transport of the lightest particles down-estuary over the salt front or along the pycnocline, and caused the salt front to move away from the heaviest particles that remained near bottom up-estuary of the salt front.

Evidence exists for negative effects of wind and flow events on striped bass egg and larval survival. Storm events have resulted in episodic mortalities of eggs and newly hatched striped bass larvae, effectively eliminating $> 50\%$ of a season's egg production in 1987 (Rutherford and Houde 1995). Drops in temperature (Uphoff 1989) and pH (Hall et al. 1985) associated with storm runoff events have a negative impact on early-stage survival. In addition to direct mortality, model results suggest that changes in circulation patterns associated with wind and river pulses could result in loss of eggs down-estuary of the ETM nursery area where poor survival could be likely (Secor et al. 1995).

Although wind and river pulse events may have a short-term negative effect on egg transport and early-stage survival, model results also indicate that circulation patterns after pulses in river flow enhance transport to the ETM nursery area. This suggests that timed spawning after river pulse events may be beneficial for early-stage survival by enhancing transport of eggs to the ETM nursery area. In addition to enhancing egg transport, spawning after pulsed events may be advantageous because increased sediment and organic matter delivery to the ETM region during the pulsed event may enhance turbidity and provide better refuge from visual predators. The pulse in organic matter may fuel copepod production, creating a zone of enhanced prey for larvae when they begin to feed.

In situ observations of striped bass egg production suggest that striped bass time spawning after peaks in river discharge. Striped bass are known to spawn in pulses (Setzler-Hamilton et al. 1981; Secor and Houde 1995), and spawn during rising water temperatures (Olney et al. 1991; Rutherford and Houde 1995; Secor and Houde 1995; Robi-

chaud-LeBlanc et al. 1996; Rutherford et al. 1997), decrease spawning during passage of cold fronts (Olney et al. 1991; Secor and Houde 1995), and reduce spawning when temperatures drop (Secor and Houde 1995) or are below 12°C (McGovern and Olney 1996). Drops in water temperature in upper estuaries during striped bass spawning season were coincident with pulses in river discharge, after which followed periods of warming temperatures (Rutherford et al. 1997). Taken together, this information suggests that striped bass may time spawning after pulses in river flow.

If beneficial conditions occur after pulses in discharge, and striped bass time their spawning to follow these events, then pulsed flow events could have a positive influence on the survival of early stage striped bass. This hypothesis is supported by the results of the multiple regression analysis with observed data from upper Chesapeake Bay. Mean spring discharge and the number of pulsed river flow events were significant effects in the model, and both had positive parameter estimates. These factors explained 71% of the variability in striped bass juvenile abundance index and suggest that the river pulse events, in addition to mean spring flow rates (as discussed in North and Houde 2001, 2003), could be an important factor controlling striped bass recruitment variability.

This modeling and data analysis effort does not encompass the intricacies of striped bass spawning behavior (vertical location of spawning, age-dependent timing of spawning; Secor 2000), egg characteristics (variation in diameter), egg development (potential change in specific gravity and diameter, temperature-dependent hatching rate), water temperature variations, wind forcing (up-estuary and cross-channel wind events), and the many different durations and timings of wind and river pulse events that occur during striped bass spawning season. It provides basic information on the potential effect of events on striped bass egg transport, increases our understanding of biological-physical interactions in striped bass early-life, and presents a hypothesis that links pulses in river discharge to recruitment variability. Examining the survival and growth of larval fish cohorts in relation to events could test this hypothesis. This research also suggests that coupled hydrodynamic-particle tracking models may be applied in other river systems to investigate if striped bass egg size and specific gravity may be an adaptation for transport to ETM nursery areas and if episodic events may have the same influence on striped bass egg transport as found for upper Chesapeake Bay. Results of this research also have management implications; anthropogenic modifications to the frequency, magnitude, and duration of pulses in river flow (e.g., dam regulation, increased impervious surfaces, global climate change) may influence striped bass egg transport and early-stage survival.

Episodic events are recurrent phenomena in estuarine, coastal and marine systems that may have an important role in influencing fisheries recruitment variability. Pulses in freshwater flow can affect circulation patterns in estuaries (Schubel and Pritchard 1986), plume dynamics at estuary mouths (Chao 1988), and, to a lesser extent, the strength of alongshore coastal currents (Chao 1987) that have significant consequences for larval transport and retention. Wind events may be important for the transport of larval fish to, and within, estuarine nursery areas (Govoni and Pietrafesa 1994; North and Houde 2004), and may mix the water column with negative or positive effects on larval fish feeding and survival (Lasker 1975; Rothschild and Osborn 1988). This research suggests that major hypotheses regarding fish recruitment variability, such as the match-mismatch (Cushing 1975) and member-vagrant (Iles and Sinclair 1982) hypotheses, should be addressed at event scales as well as at seasonal scales. Coupled 3-D hydrodynamic-particle tracking models have offered significant new insights into factors that affect larval fish survival and recruitment (e.g., Werner et al. 1996, 2001; Heath and Gallego 1998; Hare et al. 1999; Bartsch and Coombs 2001; Hinckley et al. 2001), yet many models are forced with mean wind and flow regimes (although there are exceptions, e.g., Hinrichsen et al. 2003; Brown et al. 2004). High resolution physical forcing that captures event scale processes may be the next step in numerical model development that will significantly advance our understanding of fish recruitment variability.

Acknowledgments

We thank Edward Houde, Roger Rulifson, Alan Blumberg, Victoria Coles, and Ming Li for helpful information and discussions. We also appreciate E. Houde's comments on the submitted manuscript. This research was part of the Bio-Physical Interactions in the Turbidity Maximum (BITMAX) program sponsored by an National Science Foundation Biological Oceanography Program award to S. Y. Chao, R. R. Hood, L. P. Sanford, E. D. Houde, M. R. Roman, and C. T. Friedrichs (Grant Number: OCE-0002543). This is contribution no. 3808 of the University of Maryland Center for Environmental Science, Horn Point Laboratory.

Literature Cited

Albrecht, A. B. 1964. Some observations on factors associated with survival of striped bass eggs and larvae. *California Fish and Game* 50:100–113.

Bartsch, J. and S. H. Coombs. 2001. An individual-based growth and transport model of the early life-history stages of mackerel (*Scomber scombrus*) in the eastern North Atlantic. *Ecological Modelling* 138:127–141.

Bennett, W. A., W. J. Kimmerer, and J. R. Burau. 2002. Plasticity in vertical migration by native and exotic estuarine fishes in

a dynamic low-salinity zone. *Limnology and Oceanography* 47: 1496–1507.

Bergey, L. L., R. A. Rulifson, M. L. Gallagher, and A. S. Overton. 2003. Variability of Atlantic coast striped bass egg characteristics. *North American Journal of Fisheries Management* 23: 558–572.

Blumberg, A. F. and G. L. Mellor. 1987. A description of a three-dimensional coastal ocean circulation model, p. 1–16. *In* N. Heaps (ed.), Three-dimensional Coastal Ocean Models, Volume 4. American Geophysical Union, Washington, D.C.

Boynton, W. R., W. Boicourt, S. Brant, J. Hagy, L. W. Harding, E. Houde, D. V. Holliday, M. Jech, W. M. Kemp, C. Lascara, S. D. Leach, A. P. Madden, M. Roman, L. P. Sanford, and E. M. Smith. 1997. Interactions between physics and biology in the estuarine turbidity maximum (ETM) of Chesapeake Bay, USA. International Council for the Exploration of the Sea CM 1997/S:11.

Brickman, D. and P. C. Smith. 2002. Lagrangian stochastic modeling in coastal oceanography. *Journal of Atmospheric and Ocean Technology* 19:83–99.

Brown, C. A., S. A. Holt, G. A. Jackson, D. A. Brooks, and G. J. Holt. 2004. Simulating larval supply to estuarine nursery areas: How important are physical processes to the supply of larvae to the Aransas Pass Inlet? *Fisheries Oceanography* 13:181–196.

Chao, S.-Y. 1987. Wind-driven motion near inner-shelf fronts. *Journal of Geophysical Research* 92:3849–3860.

Chao, S. Y. 1988. River-forced estuarine plumes. *Journal of Physical Oceanography* 18:72–88.

Chesney, E. J. 1989. Estimating the food-requirements of striped bass larvae *Morone saxatilis*—Effects of light, turbidity and turbulence. *Marine Ecology Progress Series* 53:191–200.

Cushing, D. 1975. Marine Ecology and Fisheries, 1st edition. Cambridge University Press, Cambridge, U.K.

Dauvin, J. C. and J. J. Dodson. 1990. Relationship between feeding incidence and vertical and longitudinal distribution of rainbow smelt larvae (*Osmerus mordax*) in a turbid well-mixed estuary. *Marine Ecology Progress Series* 60:1–12.

Dodson, J. J., J. C. Dauvin, R. G. Ingram, and B. Dangeljan. 1989. Abundance of larval rainbow smelt (*Osmerus mordax*) in relation to the maximum turbidity zone and associated macroplanktonic fauna of the middle St. Lawrence estuary. *Estuaries* 12:66–81.

Doroshev, S. I. 1970. Biological features of the eggs, larvae, and young of the striped bass (*Roccus saxatilis* (Walbaum)) in connection with the problem of its acclimatization in the USSR. *Journal of Ichthyology* 10:235–248.

Dovel, W. L. 1971. Fish eggs and larvae of the upper Chesapeake Bay. University of Maryland, NRI Special Report No. 4. Solomons, Maryland.

Geyer, W. R. and R. P. Signell. 1992. A reassessment of the role of tidal dispersion in estuaries and bays. *Estuaries* 15:97–108.

Govoni, J. J. and L. J. Pietrafesa. 1994. Eulerian views of layered water currents, vertical distribution of some larval fishes, and inferred advective transport over the continental shelf off North Carolina, USA, in winter. *Fisheries Oceanography* 3:120–132.

Hall, L. W., A. E. Pinkney, L. O. Horseman, and S. E. Finger. 1985. Mortality of striped bass larvae in relation to contaminants and water-quality in a Chesapeake Bay tributary. *Transactions of the American Fisheries Society* 114:861–868.

Hare, J. A., J. A. Quinlan, F. E. Werner, B. O. Blanton, J. J. Govoni, R. B. Forward, L. R. Settle, and D. E. Hoss. 1999. Larval transport during winter in the SABRE study area: Results of a coupled vertical behaviour-three-dimensional circulation model. *Fisheries Oceanography* 8:57–76.

Heath, M. R. and A. Gallego. 1998. Bio-physical modelling of the early life stages of haddock, *Melanogrammus aeglefinus,* in the North Sea. *Fisheries Oceanography* 7:110–125.

Hinckley, S., A. J. Hermann, K. L. Mier, and B. A. Megrey. 2001. Importance of spawning location and timing to successful transport to nursery areas: A simulation study of Gulf of Alaska walleye pollock. *ICES Journal of Marine Science* 58: 1042–1052.

Hinrichsen, H. H., U. Bottcher, F. W. Koster, A. Lehmann, and M. A. St. John. 2003. Modelling the influences of atmospheric forcing conditions on Baltic cod early life stages: Distribution and drift. *Journal of Sea Research* 49:187–201.

Iles, T. D. and M. Sinclair. 1982. Atlantic herring: Stock discreteness and abundance. *Science* 215:267–633.

Jassby, A. D., W. J. Kimmerer, S. G. Monismith, C. Armor, J. E. Cloern, T. M. Powell, J. R. Schubel, and T. J. Vendlinski. 1995. Isohaline position as a habitat indicator for estuarine populations. *Ecological Applications* 5:272–289.

Kane, A. S., R. O. Bennett, and E. B. May. 1990. Effect of hardness and salinity on survival of striped bass larvae. *North American Journal of Fisheries Management* 10:67–71.

Kimmel, D. G. and M. R. Roman. 2004. Long-term trends in mesozooplankton abundance and community composition in the Chesapeake Bay: Influence of freshwater input. *Marine Ecology Progress Series* 267:71–83.

Kimmerer, W. J., J. R. Burau, and W. A. Bennett. 1998. Tidally oriented vertical migration and position maintenance of zooplankton in a temperate estuary. *Limnology and Oceanography* 43:1697–1709.

Lal, K., R. Lasker, and A. Kuljis. 1977. Acclimation and rearing of striped bass larvae in sea water. *California Fish and Game* 63: 210–218.

Laprise, R. and J. J. Dodson. 1989. Ontogenetic changes in the longitudinal distribution of two species of larval fish in a turbid well-mixed estuary. *Journal of Fish Biology* 35:39–47.

Lasker, R. 1975. Field criteria for survival of anchovy larvae: The relation between inshore chlorophyll maximum layers and successful first feeding. *Fishery Bulletin* 73:453–462.

Mansueti, R. J. 1958. Eggs, larvae, and young of the striped bass, *Roccus saxatilis.* Maryland Department of Research and Education, Chesapeake Biological Laboratory, Solomons, Maryland.

McGovern, J. C. and J. E. Olney. 1996. Factors affecting survival of early life stages and subsequent recruitment of striped bass on the Pamunkey River, Virginia. *Canadian Journal of Fisheries and Aquatic Sciences* 53:1713–1726.

Mellor, G. L. 1998. User's guide for a three-dimensional, primitive equation, numerical ocean model, p. 44. Program in Atmospheric and Ocean Sciences, Princeton University, Princeton, New Jersey.

Mellor, G. L. and T. Yamada. 1974. A hierarchy of turbulence closure models for planetary boundary layers. *Journal of Atmospheric Science* 31:1791–1806.

Morgan, R. P., V. J. Rasin, and R. L. Copp. 1981. Temperature and salinity effects on development of striped bass eggs and larvae. *Transactions of the American Fisheries Society* 110:95–99.

North, E. W., S.-Y. Chao, L. P. Sanford, and R. R. Hood. 2004. The influence of wind and river pulses on an estuarine turbidity maximum: Numerical studies and field observations in Chesapeake Bay. *Estuaries* 27:132–146.

North, E. W. and E. D. Houde. 2001. Retention of white perch and striped bass larvae: Biological-physical interactions in Chesapeake Bay estuarine turbidity maximum. *Estuaries* 24: 756–769.

North, E. W. and E. D. Houde. 2003. Linking ETM physics, zooplankton prey, and fish early-life histories to white perch (*Morone americana*) and striped bass (*M. saxatilis*) recruitment success. *Marine Ecology Progress Series* 260:219–236.

North, E. W. and E. D. Houde. 2004. Distribution and transport of bay anchovy (*Anchoa mitchilli*) eggs and larvae in Chesapeake Bay. *Estuarine Coastal and Shelf Science* 60:409–429.

Olney, J. E., J. D. Field, and J. C. McGovern. 1991. Striped bass

egg mortality, production, and female biomass in Virginia rivers, 1980–1989. *Transactions of the American Fisheries Society* 120: 354–367.

RAUDKIVI, A. J. 1990. Loose Boundary Hydraulics, 3rd edition. Pergamon Press, Oxford, U.K.

ROBICHAUD-LEBLANC, K. A., S. C. COURTENAY, AND A. LOCKE. 1996. Spawning and early life history of a northern population of striped bass (*Morone saxatilis*) in the Miramichi River estuary, Gulf of St. Lawrence. *Canadian Journal of Zoology* 74: 1645–1655.

ROMAN, M. R., D. V. HOLLIDAY, AND L. P. SANFORD. 2001. Temporal and spatial patterns of zooplankton in the Chesapeake Bay turbidity maximum. *Marine Ecology Progress Series* 213:215–227.

ROTHSCHILD, B. J. AND T. R. OSBORN. 1988. Small-scale turbulence and plankton contact rates. *Journal of Plankton Research* 10:465–474.

RULIFSON, R. A. AND K. A. TULL. 1999. Striped bass spawning in a tidal bore river: The Shubenacadie estuary, Atlantic Canada. *Transactions of the American Fisheries Society* 128:613–624.

RUTHERFORD, E. S. AND E. D. HOUDE. 1995. The influence of temperature on cohort-specific growth, survival, and recruitment of striped bass, *Morone saxatilis,* larvae in Chesapeake Bay. *Fishery Bulletin* 93:315–332.

RUTHERFORD, E. S., E. D. HOUDE, AND R. M. NYMAN. 1997. Relationship of larval-stage growth and mortality to recruitment of striped bass, *Morone saxatilis,* in Chesapeake Bay. *Estuaries* 20:174–198.

SANFORD, L. P., W. C. BOICOURT, AND S. R. RIVES. 1992. Model for estimating tidal flushing of small embayments. *Journal of Waterway Port Coastal and Ocean Engineering-ASCE* 118:635–654.

SANFORD, L. P., S. E. SUTTLES, AND J. P. HALKA. 2001. Reconsidering the physics of the Chesapeake Bay estuarine turbidity maximum. *Estuaries* 24:655–669.

SAS INSTITUTE INC. 1997. SAS/STAT Software: Changes and Enhancements through Release 6.12. Cary, North Carolina.

SCHILLER, L. AND A. NAUMANN. 1933. Über die grundlegenden Berechnungen bei der Schwerkraftaufbereitung. Zeitschrift d. V.D.I. 77.

SCHUBEL, J. R. 1968. Turbidity maximum of northern Chesapeake Bay. *Science* 161:1013–1015.

SCHUBEL, J. R., W. CRONIN, AND G. SCHMIDT. 1974. Some observations on the sizes and settling velocities of fish eggs. The Johns Hopkins University, Chesapeake Bay Institute, Baltimore, Maryland.

SCHUBEL, J. R. AND D. W. PRITCHARD. 1986. Responses of upper Chesapeake Bay to variations in discharge of the Susquehanna River. *Estuaries* 9:236–249.

SECOR, D. H. 2000. Spawning in the nick of time? Effect of adult demographics on spawning behavior and recruitment in Chesapeake Bay striped bass. *ICES Journal of Marine Science* 57: 403–411.

SECOR, D. H. AND E. D. HOUDE. 1995. Temperature effects on the timing of striped bass egg-production, larval viability, and recruitment potential in the Patuxent River (Chesapeake Bay). *Estuaries* 18:527–544.

SECOR, D. H., E. D. HOUDE, AND D. M. MONTELEONE. 1995. A mark-release experiment on larval striped bass *Morone saxatilis* in a Chesapeake Bay tributary. *ICES Journal of Marine Science* 52:87–101.

SETZLER-HAMILTON, E. M., W. R. BOYNTON, J. A. MIHURSKY, T. T. POLGAR, AND K. V. WOOD. 1981. Spatial and temporal distribution of striped bass eggs, larvae and juveniles in the Potomac estuary. *Transactions of the American Fisheries Society* 110: 121–136.

SETZLER-HAMILTON, E. M. AND L. HALL, JR. 1991. Striped bass, *Morone saxatilis,* p. 13-11 to 13-31. *In* S. L. Funderburk, S. J. Jordan, J. A. Mihursky, and D. Riley (eds.), Habitat Requirements for Chesapeake Bay Living Resources. Chesapeake Bay Program, Annapolis, Maryland.

SIMENSTAD, C. A., C. A. MORGAN, J. R. CORDELL, AND J. A. BAROSS. 1994. Flux, passive retention and active residence of zooplankton in Columbia River estuarine turbidity maxima, p. 473–482. *In* K. R. Dyer and R. J. Orth (eds.), Changes in Fluxes in Estuaries: Implications from science to management. Olsen and Olsen, Fredensborg, Denmark.

SIROIS, P. AND J. J. DODSON. 2000. Critical periods and growth-dependent survival of larvae of an estuarine fish, the rainbow smelt *Osmerus mordax. Marine Ecology Progress Series* 203:233–245.

UPHOFF, J. H. 1989. Environmental effects on survival of eggs, larvae, and juveniles of striped bass in the Choptank River, Maryland. *Transactions of the American Fisheries Society* 118:251–263.

VISSER, A. W. 1997. Using random walk models to simulate the vertical distribution of particles in a turbulent water column. *Marine Ecology Progress Series* 158:275–281.

WALDMAN, J. R., K. NOLAN, J. HART, AND I. I. WIRGIN. 1996. Genetic differentiation of three key anadromous fish populations of the Hudson River. *Estuaries* 19:759–768.

WERNER, F. E., B. R. MACKENZIE, R. I. PERRY, R. G. LOUGH, C. E. NAIMIE, B. O. BLANTON, AND J. A. QUINLAN. 2001. Larval trophodynamics, turbulence, and drift on Georges Bank: A sensitivity analysis of cod and haddock. *Scientia Marina* 65:99–115.

WERNER, F. E., R. I. PERRY, R. G. LOUGH, AND C. E. NAIMIE. 1996. Trophodynamic and advective influences on Georges Bank larval cod and haddock. *Deep-Sea Research* 43:1793–1822.

WINGER, P. V. AND P. J. LASIER. 1994. Effects of salinity on striped bass eggs and larvae from the Savannah River, Georgia. *Transactions of the American Fisheries Society* 123:904–912.

WINKLER, G., J. J. DODSON, N. BERTRAND, D. THIVIERGE, AND W. F. VINCENT. 2003. Trophic coupling across the St. Lawrence River estuarine transition zone. *Marine Ecology Progress Series* 251:59–73.

Received, June 15, 2004
Accepted, September 13, 2004